

A pair of diastereomeric 1:1 salts of (*S*)- and (*R*)-2-methylpiperazine with (*2S,3S*)-tartaric acid

Hiroshi Katagiri,^{a*} Masao Morimoto^b and Kenichi Sakai^b

^aDepartment of Chemistry and Chemical Engineering, Graduate School of Science and Engineering, Yamagata University, 4-3-16 Jonan, Yonezawa, Yamagata 992-8510, Japan, and ^bSpecialty Chemicals Technology Development Department, Toray Fine Chemicals Co. Ltd, Minato-ku, Nagoya, Aichi 455-8502, Japan
Correspondence e-mail: kgri7078@yz.yamagata-u.ac.jp

Received 11 May 2009

Accepted 23 June 2009

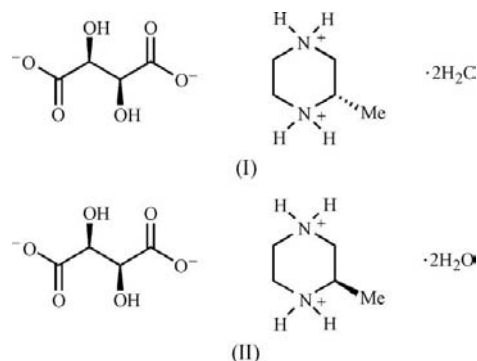
Online 30 June 2009

The structures of diastereomeric pairs consisting of (*S*)- and (*R*)-2-methylpiperazine with (*2S,3S*)-tartaric acid are both 1:1 salts, namely (*S*)-2-methylpiperazinium (*2S,3S*)-tartrate dihydrate, $C_5H_{14}N_2^{2+} \cdot C_4H_4O_6^{2-} \cdot 2H_2O$, (I), and (*R*)-2-methylpiperazinium (*2S,3S*)-tartrate dihydrate, $C_5H_{14}N_2^{2+} \cdot C_4H_4O_6^{2-} \cdot 2H_2O$, (II), which reveal the formation of well defined ammonium carboxylate salts linked *via* strong intermolecular hydrogen bonds. Unlike the situation in the more soluble salt (II), the alternating columns of tartrate and ammonium ions of the less soluble salt (I) are packed neatly in a grid around the *a* axis, which incorporates water molecules at regular intervals. The increased efficiency of packing for (I) is evident in its lower 'packing coefficient', and the hydrogen-bond contribution is stronger in the more soluble salt (II).

Comment

Tartaric acid is one of the most accessible enantiomerically pure compounds, and it has emerged as a useful class of chiral resolving reagents for racemic amines (Gawronski & Gawronska, 1999). Although a variety of amines have been resolved by the formation of diastereomeric salts with tartaric

acid, systematic research on the crystal structures of diastereomers is still of importance if the process is to become nonheuristic. We report here the crystal structures of a pair of diastereomeric 1:1 salts, (I) and (II), of (*2S,3S*)-tartaric acid with (*S*)- and (*R*)-2-methylpiperazine, respectively; (*R*)-2-methylpiperazine is a valuable compound as a raw material for various drugs and candidates for clinical compounds designed to treat HIV infection (Gala *et al.*, 2003), obesity (Chen *et al.*, 2006), hypertension (Bell *et al.*, 2004) and diabetes (Cernerud *et al.*, 2004).



In both crystal structures, the N atoms of 2-methylpiperazine each have two H atoms, showing that these amines are completely converted to quaternary ammonium cations (Figs. 1 and 2). It is also found that the O3—C6, O4—C6, O5—C9 and O6—C9 bond lengths of the tartrate ions lie between 1.2416 (15) and 1.2811 (16) Å (Tables 1 and 3), which means that the O—C bonds are longer than the standard double bond of a carboxylic acid (1.200 Å) but shorter than a single bond (1.317 Å) (Leiserowitz, 1976), indicating the formation of well defined carboxylate anions. In addition, the geometries of the 2-methylpiperazinium ions are almost identical except for the configuration at C4. The torsion angles C1—N1—C4—C5 in (I) and C1—N2—C4—C5 in (II) are 178.47 (10) and 176.85 (10)°, respectively, indicating that these methyl groups are in the most stable equatorial position in the chair conformation of the piperazine ring. The conformations of the tartrate ions also have roughly the same geometry around the C7—C8 axis, and the O1—C7—C8—O2 torsion angle is 67.06 (13) in (I) and 70.93 (12)° in (II).

In the crystal packing, the molecules are linked *via* strong intermolecular O—H...O and N—H...O hydrogen bonds (Figs. 3 and 4, and Tables 2 and 4). The crystal packing of (I) reveals neat alternating columns of tartrate and ammonium

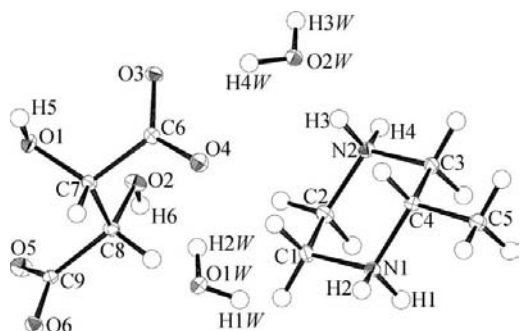


Figure 1

The asymmetric unit of (I), showing 50% probability displacement ellipsoids. H atoms are shown as spheres.

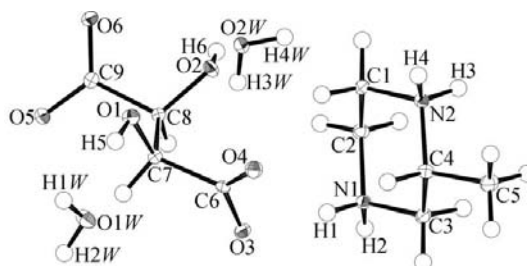


Figure 2

The asymmetric unit of (II), showing 50% probability displacement ellipsoids. H atoms are shown as spheres.

ions in a grid around the *a* axis that incorporates water molecules at regular intervals, whereas in (II) the columns are more interconnected. The solubility of 5.0 g/100 g H₂O for (I) is less than that of 63.6 g/100 g H₂O for (II) at 298 K, and the crystal density of 1.523 Mg m⁻³ for (I) is greater than that of 1.493 Mg m⁻³ for (II). The increased efficiency of packing for (I) is also evident in its lower ‘packing coefficient’ (Spek, 2009)

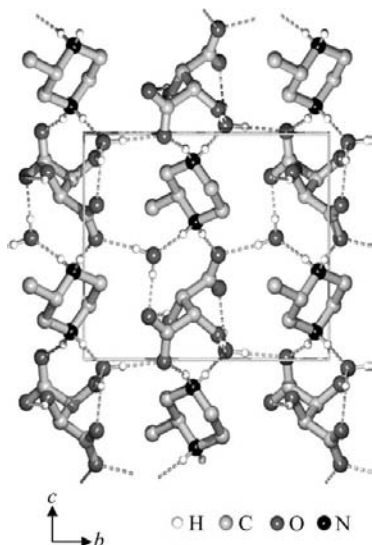


Figure 3
The packing of (I) along the *a* axis, showing neat alternating columns of tartrate and ammonium ions in a grid around the *a* axis that incorporates water molecules at regular intervals.

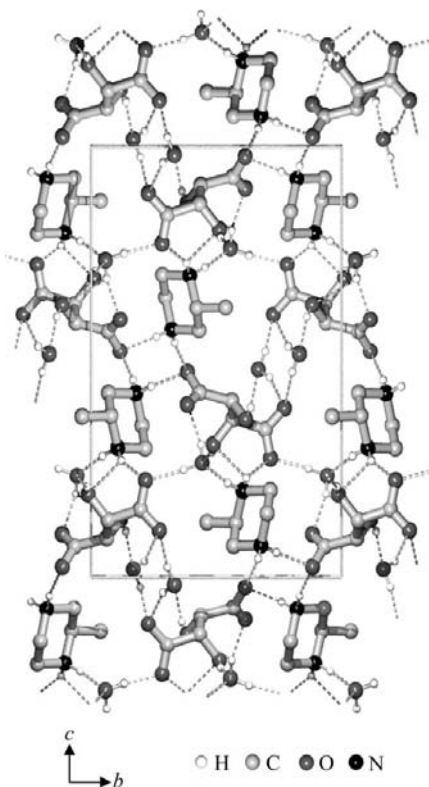


Figure 4
The packing of (II) along the *a* axis, showing the columns of tartrate and ammonium ions interconnected by hydrogen bonds.

(77.1%), which differs by 2.4% from the value found for (II) (75.3%), indicating the presence of a stronger intermolecular interaction in the less soluble salt (I). In contrast, there are more hydrogen bonds in (II) than in (I). Additionally, a scatter diagram of angles (*D*–H···*A*) versus distances (H···*A*) for individual intermolecular hydrogen bonds shows two weak hydrogen bonds in (I), which correspond to the interactions of hydroxy groups with a symmetry-related carboxylate group and a water molecule (Figs. 5 and 6). These hydrogen bonds form columns of tartrate ions around the *a* axis in (I). On the other hand, as shown in Fig. 7, the two weakest hydrogen bonds in (II) take the form of bifurcated hydrogen bonds, whose values are estimated as being weaker than those of ordinary hydrogen bonds constituted geometrically with a single donor and an acceptor. From the number of hydrogen bonds and the correlation between length and angle, we predict that these interactions are stronger in the more soluble salt (II). Although the less soluble diastereomeric salts are commonly stabilized by intermolecular interactions to a much greater extent than the corresponding more soluble diastereomeric salts, it has been reported that the number of hydrogen bonds does not necessarily lead to greater stability and less solubility in hydrated salts (Langkilde *et al.*, 2002). Therefore, other than hydrogen bonds, Coulombic interactions and van der Waals interactions make a large contribution to the stabilization of the packing structure of the less soluble salt (I). In contrast, the more soluble salt (II) is structurally disadvantaged in close packing, and adopts the less stable packing structure supported by intermolecular hydrogen bonds.

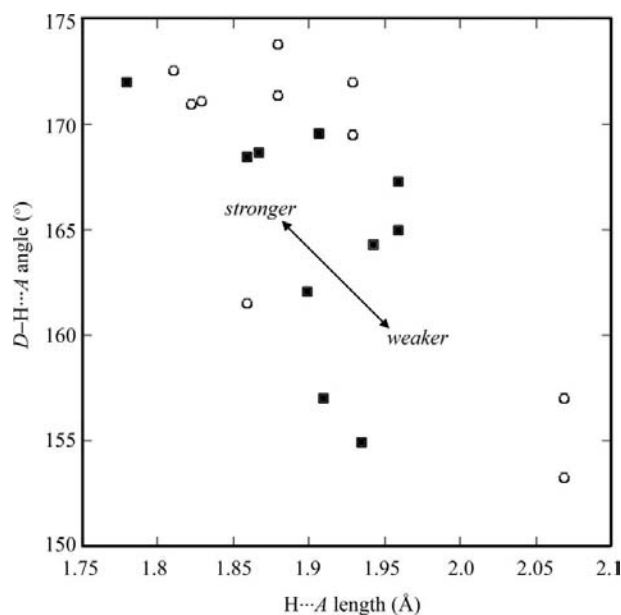


Figure 5
Scatter plot of angles (*D*–H···*A* > 150°) versus distances (H···*A*) for intermolecular hydrogen bonds in (I) (open circles) and in (II) (black squares), showing the strength of the individual hydrogen bonds. The O2W–H3W···O1 and N2–H4···O2^{iv} bonds (see Table 4) in (II) have been omitted owing to their obvious weakness.

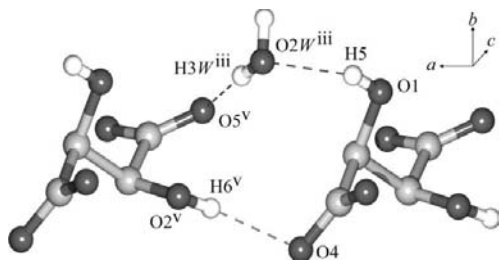


Figure 6
A perspective view of the partial packing of (I), showing two weaker hydrogen bonds which correspond to the interactions of hydroxy groups attached to a symmetry-related carboxylate group and a water molecule. [Symmetry codes: (iii) $-x + 1, y + \frac{1}{2}, -z$; (v) $1 + x, y, z$.]

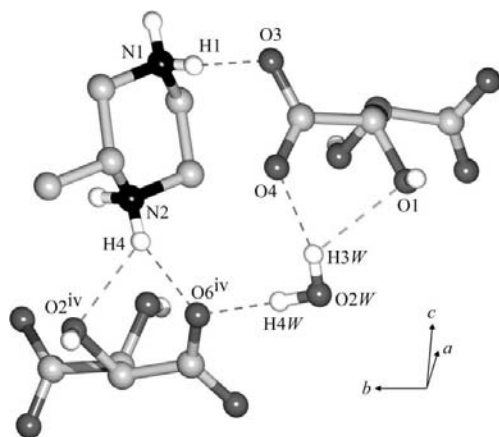


Figure 7
A perspective view of the partial packing of (II), showing the weaker two hydrogen bonds adopted as bifurcated hydrogen bonds. [Symmetry code: (iv) $-x + 1, y + \frac{1}{2}, -z + \frac{3}{2}$.]

Experimental

Enantiomeric pure (2*S*,3*S*)-tartaric acid and (*S*)- and (*R*)-2-methylpiperazine were manufactured by Toray Fine Chemicals Co. Ltd (Japan). Both salts were prepared by heating 1 mmol quantities of (2*S*,3*S*)-tartaric acid and (*S*)-2-methylpiperazine [for (I)] or (*R*)-2-methylpiperazine [for (II)] under reflux in water. Subsequent cooling to room temperature afforded a crop of colourless prisms [m.p. 518–519 K for (I) and 498–499 K for (II)]. Their melting points were measured on a melting point apparatus. The solubility of these salts in water was established by the equilibration method, *i.e.* preparation of a saturated solution at room temperature and determination of its concentration.

Compound (I)

Crystal data

$C_5H_{14}N_2^{2+} \cdot C_4H_4O_6^{2-} \cdot 2H_2O$
 $M_r = 286.29$
 Monoclinic, $P2_1$
 $a = 6.0830$ (9) Å
 $b = 10.8648$ (16) Å
 $c = 9.6826$ (14) Å
 $\beta = 102.621$ (5)°

$V = 624.47$ (16) Å³
 $Z = 2$
 Mo $K\alpha$ radiation
 $\mu = 0.13$ mm⁻¹
 $T = 123$ K
 $0.60 \times 0.60 \times 0.20$ mm

Data collection

Rigaku R-Axis RAPID
 diffractometer
 Absorption correction: multi-scan
 (ABSCOR; Higashi, 1995)
 $T_{min} = 0.924, T_{max} = 0.974$

10636 measured reflections
 1507 independent reflections
 1502 reflections with $I > 2\sigma(I)$
 $R_{int} = 0.022$

Refinement

$R[F^2 > 2\sigma(F^2)] = 0.020$
 $wR(F^2) = 0.050$
 $S = 1.05$
 1507 reflections
 214 parameters
 1 restraint

H atoms treated by a mixture of independent and constrained refinement
 $\Delta\rho_{max} = 0.24$ e Å⁻³
 $\Delta\rho_{min} = -0.15$ e Å⁻³

Table 1

Selected geometric parameters (Å, °) for (I).

O3—C6	1.2605 (15)	O5—C9	1.2416 (15)
O4—C6	1.2580 (16)	O6—C9	1.2718 (15)
C1—N1—C4—C5	178.47 (10)	O1—C7—C8—O2	67.06 (13)

Table 2

Hydrogen-bond geometry (Å, °) for (I).

<i>D</i> —H... <i>A</i>	<i>D</i> —H	H... <i>A</i>	<i>D</i> ... <i>A</i>	<i>D</i> —H... <i>A</i>
N1—H1...O1W ⁱ	0.943 (19)	1.83 (2)	2.7657 (15)	171.1 (18)
N1—H2...O6 ⁱ	0.894 (19)	1.811 (19)	2.7004 (15)	172.6 (17)
N2—H3...O2W	0.93 (2)	1.88 (2)	2.7981 (15)	171.4 (18)
N2—H4...O3 ⁱⁱ	0.927 (19)	1.86 (2)	2.7565 (15)	161.5 (18)
O1W—H1W...O6 ⁱ	0.84 (2)	1.93 (2)	2.7523 (14)	169.5 (19)
O1W—H2W...O4	0.889 (19)	1.823 (19)	2.7043 (14)	171.0 (19)
O2W—H3W...O5 ⁱⁱ	0.80 (3)	1.93 (3)	2.7189 (13)	172 (3)
O2W—H4W...O3	0.87 (2)	1.88 (2)	2.7454 (14)	173.8 (18)
O1—H5...O2W ⁱⁱⁱ	0.81 (2)	2.07 (2)	2.8340 (14)	157 (2)
O2—H6...O4 ^{iv}	0.84 (2)	2.07 (2)	2.8486 (14)	153.3 (19)

Symmetry codes: (i) $-x + 1, y - \frac{1}{2}, -z + 1$; (ii) $-x, y - \frac{1}{2}, -z$; (iii) $-x + 1, y + \frac{1}{2}, -z$; (iv) $x - 1, y, z$.

Compound (II)

Crystal data

$C_5H_{14}N_2^{2+} \cdot C_4H_4O_6^{2-} \cdot 2H_2O$
 $M_r = 286.29$
 Orthorhombic, $P2_12_12_1$
 $a = 6.1303$ (2) Å
 $b = 11.3207$ (5) Å
 $c = 18.3570$ (5) Å

$V = 1273.96$ (8) Å³
 $Z = 4$
 Mo $K\alpha$ radiation
 $\mu = 0.13$ mm⁻¹
 $T = 108$ K
 $0.60 \times 0.60 \times 0.60$ mm

Data collection

Rigaku R-Axis RAPID
 diffractometer
 Absorption correction: multi-scan
 (ABSCOR; Higashi, 1995)
 $T_{min} = 0.926, T_{max} = 0.926$

12586 measured reflections
 1697 independent reflections
 1670 reflections with $I > 2\sigma(I)$
 $R_{int} = 0.016$

Refinement

$R[F^2 > 2\sigma(F^2)] = 0.022$
 $wR(F^2) = 0.060$
 $S = 1.05$
 1697 reflections
 212 parameters

H atoms treated by a mixture of independent and constrained refinement
 $\Delta\rho_{max} = 0.31$ e Å⁻³
 $\Delta\rho_{min} = -0.18$ e Å⁻³

Table 3

Selected geometric parameters (Å, °) for (II).

O3—C6	1.2811 (16)	O5—C9	1.2581 (15)
O4—C6	1.2408 (16)	O6—C9	1.2575 (15)
C1—N2—C4—C5	176.85 (10)	O1—C7—C8—O2	70.93 (12)

Table 4

Hydrogen-bond geometry (Å, °) for (II).

<i>D</i> —H... <i>A</i>	<i>D</i> —H	H... <i>A</i>	<i>D</i> ... <i>A</i>	<i>D</i> —H... <i>A</i>
N1—H1...O3	0.885 (19)	1.86 (2)	2.7344 (15)	168.5 (18)
N1—H2...O3 ⁱⁱ	0.875 (19)	1.908 (18)	2.7730 (15)	169.6 (17)
N2—H3...O2W ^{iv}	0.921 (19)	1.868 (18)	2.7772 (14)	168.7 (17)
N2—H4...O2 ^{iv}	0.916 (18)	2.337 (19)	2.9917 (15)	128.3 (16)
N2—H4...O6 ^{iv}	0.916 (18)	1.936 (19)	2.7926 (15)	154.9 (18)
O1W—H1W...O5 ⁱ	0.86 (2)	1.91 (2)	2.7234 (14)	157 (2)
O1W—H2W...O5 ⁱⁱⁱ	0.87 (2)	1.90 (2)	2.7401 (13)	162.1 (17)
O2W—H3W...O1	0.84 (2)	2.50 (2)	3.0201 (13)	120.8 (18)
O2W—H3W...O4	0.84 (2)	1.96 (2)	2.7802 (13)	165 (2)
O2W—H4W...O6 ^{iv}	0.90 (2)	1.78 (2)	2.6774 (13)	172 (2)
O1—H5...O1W	0.781 (18)	1.944 (18)	2.7032 (14)	164.3 (18)
O2—H6...O2W ^v	0.82 (2)	1.96 (2)	2.7671 (14)	167.3 (17)

Symmetry codes: (i) $x - 1, y, z$; (ii) $x + \frac{1}{2}, -y + \frac{3}{2}, -z + 2$; (iii) $x - \frac{1}{2}, -y + \frac{1}{2}, -z + 2$; (iv) $-x + 1, y + \frac{1}{2}, -z + \frac{3}{2}$; (v) $x + 1, y, z$.

In the refinement of (I), the positions of the alcohol, ammonium and water H atoms were determined by differential Fourier analysis near atoms O1, O2, N1, N2, O1W and O2W, and then refined isotropically. In the refinement of (II), the positions of the alcohol, ammonium and water H atoms were determined by differential Fourier analysis near atoms O1, O2, N1, N2, O1W and O2W, and then refined isotropically, except for the alcohol H atoms, which were refined with a $U_{\text{iso}}(\text{H})$ value of $1.5U_{\text{eq}}(\text{O})$. The positions of all other H atoms in both compounds were calculated geometrically and refined as riding, with C—H bond lengths of 0.98–1.00 Å, and with $U_{\text{iso}}(\text{H})$ values of 1.2 or, in the case of methyl groups, 1.5 times $U_{\text{eq}}(\text{C})$. In both

(I) and (II), in the absence of significant anomalous scattering effects, Friedel pairs were merged, and the absolute configuration was assigned from the known configuration of (2*S*,3*S*)-tartaric acid.

For both compounds, data collection: *PROCESS-AUTO* (Rigaku, 1998); cell refinement: *PROCESS-AUTO*; data reduction: *Crystal-Structure* (Rigaku/MS, 2003); program(s) used to solve structure: *SHELXS97* (Sheldrick, 2008); program(s) used to refine structure: *SHELXL97* (Sheldrick, 2008); molecular graphics: *ORTEPIII* (Burnett & Johnson, 1996) and *PLATON* (Spek, 2009); software used to prepare material for publication: *SHELXL97* and *PLATON*.

Supplementary data for this paper are available from the IUCr electronic archives (Reference: EG3019). Services for accessing these data are described at the back of the journal.

References

- Bell, A. S., Brown, D. G., Fox, D. N. A., Marsh, I. R., Morrell, A. I., Palmer, M. J. & Winslow, C. A. (2004). Patent No. WO2004096810.
- Burnett, M. N. & Johnson, C. K. (1996). *ORTEPIII*. Report ORNL-6895. Oak Ridge National Laboratory, Tennessee, USA.
- Cernerud, M., Lundstroem, H., Loeffstroem, C., Pelcman, M., Fleck, T., Paptchikhine, A., Andersson, E. & Nygren, A. (2004). Patent No. WO2004000829.
- Chen, H., Coffey, S. B., Lefker, B. A. & Liu, K. K.-C. (2006). Patent No. WO2006103511.
- Gala, D., Goodman, A. J., Lee, G., Liao, H., Schwartz, M. L., Tang, S., Tsai, D. J. S. & Wu, W. (2003). Patent No. WO2003048153.
- Gawronski, J. & Gawronska, K. (1999). In *Tartaric and Malic Acids in Synthesis: A Source Book of Building Blocks, Ligands, Auxiliaries and Resolving Agents*. New York, Chichester, Brisbane, Toronto: John Wiley and Sons.
- Higashi, T. (1995). *ABSCOR*. Rigaku Corporation, Tokyo, Japan.
- Langkilde, A., Oddershede, J. & Larsen, S. (2002). *Acta Cryst.* **B58**, 1044–1050.
- Leiserowitz, L. (1976). *Acta Cryst.* **B32**, 775–802.
- Rigaku (1998). *PROCESS-AUTO*. Rigaku Corporation, Tokyo, Japan.
- Rigaku/MS (2003). *CrystalStructure*. Version 3.6.0. Rigaku/MS, The Woodlands, Texas, USA.
- Sheldrick, G. M. (2008). *Acta Cryst.* **A64**, 112–122.
- Spek, A. L. (2009). *Acta Cryst.* **D65**, 148–155.